3D Optical Spectroscopic Methods in Astronomy
ASP Conference Series, Vol. 71, 1995
G. Comte, M. Marcelin, eds.

Impact of nuclear activity on extended emission line regions of nearby galaxies

E. Pécontal, P. Ferruit

Observatoire de Lyon, 69561 Saint-Genis-Laval Cedex, France

A.S. Wilson

Space Telescope Science Institute, Baltimore, MD21218, USA

Abstract. We used the integral field TIGER to map the intensity ratios of emission lines and the velocity field over the narrow emission line of a few nearby Seyfert galaxies. Our aim is to study the impact of nuclear activity on galaxies, which will hopefully help us to probe the central engine. We present here some results for two objects: M 51 and NGC 5929.

1. Introduction

An active nucleus interacts with its surrounding galaxy mainly by two ways: photoionization of the gas by the central UV-X source, and impact of material ejection on the interstellar medium. Usually, this material is ejected as plasma jets or bubbles (e.g. Wilson and Ulvestad 1983, Smith et al. 1983) , emitting synchrotron radiation detected in radio wavelengths. It is now well known that in many Seyfert galaxies, the radio morphology is correlated with the narrow emission line region geometry (Haniff, Wilson and Ward 1988). Emission lines ratio maps suggest that this correlation is due to the anisotropy of the ionizing flux, which would be preferentially emitted in the direction of the radio axis (Pogge 1988, Tadhunter and Tsvetanov 1989, Wilson and Baldwin 1992). The radio ejecta also influence on the kinematics of the forbidden emission-line regions (Whittle et al. 1988), and possibly the ionizing state of the gas.
We started an observing program of nearby Seyfert galaxies with the integral spectrograph TIGER (presented elsewhere in these proceedings). We present here preliminary results of the April 1992 run during which the following objects were observed: M 51 and NGC 5929, 1 hour exposures in [NII] Hα, [SII].

2. M 51

M 51 is at the lowest level of activity in Seyfert galaxies. Its radio continuum morphology (λ-6cm and λ-20cm) consists in a central peak, an extranuclear cloud (XNC) at 4" south of the nucleus and a broken ring 9" north (Ford et al. 1985). These latter authors showed that the emission line image exhibits a counterpart to the radio XNC, and suggests that the XNC could be the working

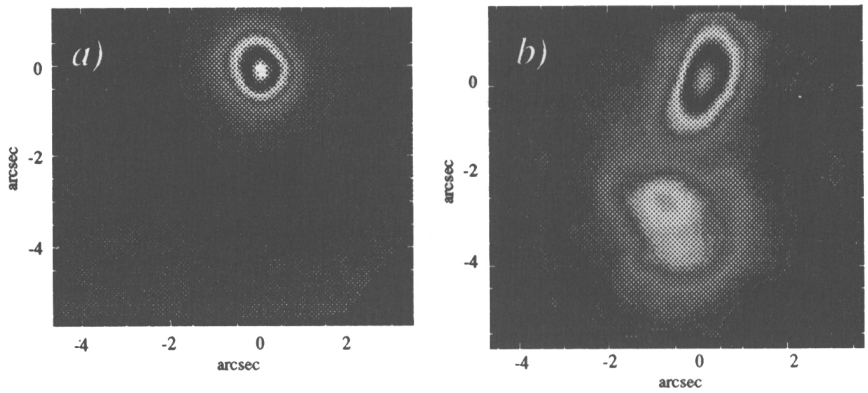

Figure 1. M51 reconstructed images. a) continuum. b) [NII]+Hα

surface of a shock between a nuclear jet and the disk gas. Cecil (1988) obtained the first 2D spectrography in Fabry-Perot spectrography of the nuclear region of M51. This study confirmed the fact that the XNC is the termini of hydrodynamics flows. Recently, new 6cm observations (Crane and Van der Hulst 1992) showed that the nuclear peak and the XNC are connected by a jetlike feature. This was the first direct observation of the jet itself. We show in Fig.1 the reconstructed images in continuum and in [NII]+Hα.

The absolute centering of the images was obtained by comparison of our continuum image with the convolved continuum HST image. The velocity slices through the [NII] line is presented in Fig.2.

Our high resolution data show that the red wing image of the XNC splits into three knots distinct from the blue wing image one. Further analysis of the data are needed to understand the nature of these knots (higher density or higher excitation regions). We perform a kinematical decomposition of the [NII] profile, following the three components decomposition proposed by Cecil. Fig.3 presents the three components maps, with the 6cm radio map of Crane and van der Hulst overimposed. As pointed out by Cecil (1988), the nuclear elongation varies with velocity. The red wing is clearly elongated in the direction of the radio jet. A difference from Cecil's data is that the systemic component is exactly coincident with the radio emission (the centering is obtained assuming that the center of the HST image is coincident with the radio central peak). This implies a low velocity shock propagation, since it covers a small distance during the cooling time of the gas.

3. NGC 5929

NGC 5929 is a well studied Seyfert galaxy, for it is the archetype for the plasmon models. Its radio source has a two-component structure (Ulvestad and Wilson 1984), the two radio lobes having an optical counterpart (Whittle et al. 1986). Furthermore, each lobe corresponds to a kinematical component in [OIII] line. Until the HST observation, it was thought that the [OIII] peaks were closer to

https://doi.org/10.1017/S0252921100023113 Published online by Cambridge University Press

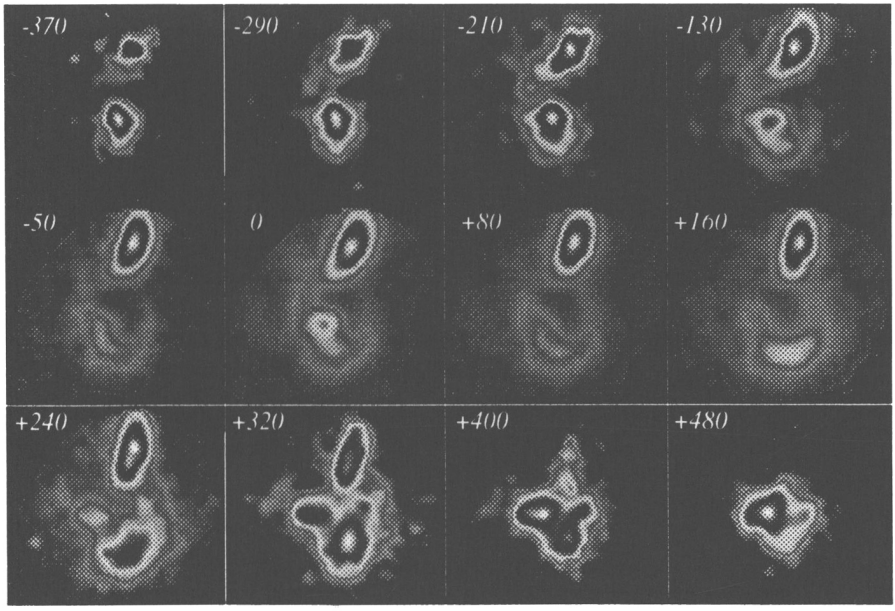

Figure 2. M51 Velocity slices of [NII] line

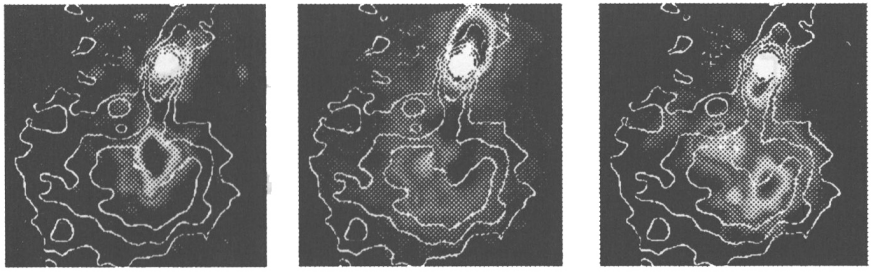

blue component narrow component red component

Figure 3. M51. Maps of the three kinematics components. 6cm map of Crane and van der Hulst overimposed

https://doi.org/10.1017/S0252921100023113 Published online by Cambridge University Press

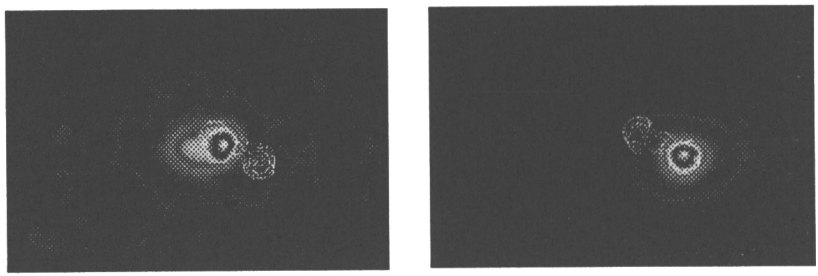

Figure 4. NGC 5929. Maps of the two kinematical components in [NII]. 6cm maps of Ulvestad and Wilson overimposed.

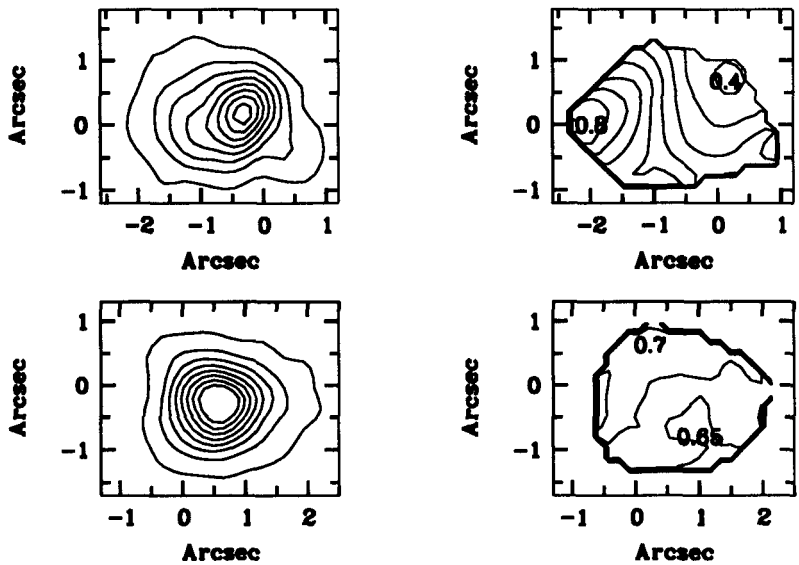

Figure 5. NGC 5929. Left: Hα intensity maps (top: east lobe, bottom: west blob). Right: [NII]/Hα maps (top: east lobe, bottom: west blob)

https://doi.org/10.1017/S0252921100023113 Published online by Cambridge University Press

the nucleus than the radio components. Bower et al. (1994) show however that there was a tight correlation between the position of the radio and emission-line peaks. Fig. 4 shows the kinematical decomposition of the two lobes. The two regions are resolved and the derived [NII]/Hα maps are displayed in Fig. 5. As can be seen in this figure, the west blob shows no variation in the [NII]/Hα ratio, though the east blob presents a strong variation of this ratio. This suggests that this cloud is composed of several blobs with different exciting mechanisms. This is confirmed by the high resolution HST image which shows that it is splited into two distinct clouds (Bower et al. 1994).

Discussion

J. Bland-Hawthorn: In many of the TIGER pictures, one gets the impression of correlated noise across the field. Please explain how you flatfield the response of the multi-lens array.

E. Pécontal: The images that are presented here are oversampled to make them more readible. The noise seems then correlated due to this oversampling. The flat-field correction is obtained as in long-slit spectrography using a dome exposure. The CCD response is multiplied by the lens-to-lens transmission and the correction of these two effects are thus simultaneous.

S. Bensammar: Could you precise the initial sampling you use and the final angular resolution you obtain after data processing?

E. Pécontal: The spatial sampling is 0.16 arcsec per pixel in imagery mode and 0.39 arcsec per pixel in spectrographic mode. For the data presented here, the spatial resolution of the data cube is 0.8".

References

Bower, G.A., Wilson, A.S., Mulchaey, J.S., Miley, G.K., Heckman, T.M., & Krolik, J.H. 1994, AJ, 105, 1686

Cecil, G. 1988, ApJ, 329, 38

Crane, P.C., & van der Hulst, J.M. 1992, AJ, 103, 1146

Ford, H.C., Crane, P.C., Jacoby, G.H., Lawrie, D. & van der Hulst, J.M. 1985, ApJ, 293, 132

Haniff, C.A., Wilson, A.S. & Ward 1988, ApJ, 334, 121

Pogge, R.W. 1988, ApJ, 332, 702

Smith, M.D., Smarr, L., Norman, M.L. & Wilson, J.R. 1983, ApJ, 264, 759 J.

Tadhunter, C., & Tsvetanov, Z. 1989 Nature, 321, 422

Ulvestad, J.S., & Wilson, A.S. 1983, ApJ, 285, 439

Whittle, M., Haniff, C.A., Ward, M.J., Pedlar, A., Unger, S.W., Axon, D.J., & Harrison, B.A. 1986, MNRAS, 222, 189

Whittle, M., Pedlar, A., Meurs, E.J.A., Unger, S.W., Axon, D.J.. & Ward, M.J. 1988, ApJ, 326, 125

Wilson, A.S., & Ulvestad, J.S. 1983 ApJ, 275, 8